

A HIGH ACTIVITY ZEOLITE-SUPPORTED COBALT FISCHER-TROPSCH CATALYST

R.R.FRAME, S.A.BRADLEY, E.SCHUMACHER AND H.B.GALA
UOP
50 EAST ALGONQUIN ROAD
DES PLAINES, IL 60017-5016

KEYWORDS: Y ZEOLITE/COBALT FISCHER-TROPSCH CATALYST
FIXED-BED TESTS
SLURRY AUTOCLAVE TESTS

Cobalt-based Fischer-Tropsch (F-T) catalysts are currently in favor because they are useful for processing methane-derived synthesis gas. There is an excess of methane at remote sites that might be economically converted into liquid hydrocarbons by a processing scheme based on F-T. Shell is purported to use a cobalt-based catalyst at their F-T plant in Sarawak. Exxon has worked extensively on supported cobalt F-T catalysts, particularly ones supported on titanium dioxide. Gulf-Chevron^{1,2,3,4} and Exxon^{5,6} have demonstrated that small amounts of ruthenium added to a supported cobalt F-T catalyst can cause catalyst activation.

Work done under a current DOE contract to UOP has resulted in a high activity, zeolite-supported, cobalt F-T catalyst (Contract No. DE-AC22-89PC8969). This catalyst resulted from impregnation of cobalt onto a Y zeolite-derived support. This support had been used in an earlier contract by workers from Union Carbide to prepare a less active cobalt F-T catalyst.

The support results from steaming and acid-washing Y zeolite. The purpose of the steaming is to create large amorphous pores in an otherwise crystalline matrix. The subsequent acid-washing removes alumina debris resulting from steaming thus clearing the remaining crystalline channels to facilitate diffusion of reactants and products to and from the catalyst active sites.

Compared to the catalyst developed during the previous Union Carbide contract, catalysts from the current work have higher cobalt levels. Thus Figure 1 illustrates the actual metals loading in some of the current catalysts compared to a reference catalyst remaining from the earlier work:

Catalysts prepared during this work were analyzed by scanning transmission electron microscopy (STEM). These analyses showed that at least some of the cobalt exists outside of the zeolite pores in crystallites attached to the external surface of the zeolite.

Short catalyst screening runs were performed in a fixed-bed pilot plant. In addition, one active catalyst was also evaluated in a longer run in a slurry autoclave pilot plant. Such a plant is useful for evaluating catalysts being developed for liquid phase F-T (LPFT) processing. The slurry autoclave run allowed determination of the catalyst deactivation rate and the change in selectivities as a function of time on stream.

When the fixed-bed reactor was used quartz sand was loaded with the catalyst to facilitate heat transfer since the F-T reactions are very exothermic. Prior to starting a run the metal oxide was reduced for two hours at 350° C with flowing hydrogen. Following reduction the reactor temperature was reduced until the inlet temperature was 211° C; the feed was then introduced. The feed rate was 4.9 NL/hour · g of cobalt and the plant pressure was 287 psig. The feed was a pure blend of hydrogen, carbon monoxide and argon purchased from Scott Specialty Gas Co. The feed molar ratio of hydrogen to carbon monoxide was two which is the same as that of a methane-derived synthesis gas. Argon was present as an internal standard for calculation of conversions and selectivities.

Figure 2 contains a tabular summary of Run 65 (reference catalyst from the previous contract) and Run 97 which used a catalyst containing about twice as much cobalt as the reference catalyst. The higher conversion during Run 97 was due, at least in part, to the *de-facto* higher operating temperature during this run (actual catalyst bed temperature profiles are in Figure 3). The high temperature resulted from the high density of active sites on the high cobalt catalyst which, in turn, caused extensive conversion near the inlet of the catalyst bed and, therefore, significant heat as well. Since cobalt-catalyzed F-T is very sensitive to temperature even a small difference between operating temperatures such as in Runs 65 and 97 can result in a significant conversion difference in

conversion. Subsequent runs with even higher cobalt catalysts used less catalyst, however, due to operational problems the amount used in these latter runs is as little as may be used.

A fresh sample of the catalyst used in Run 97 was bound with silica in preparation for use in the slurry autoclave pilot plant. For use in (LPFT) the powdery zeolite catalyst would have to be bound in order to form particulates large enough to have the required hydrodynamic properties. The bound catalyst was evaluated in the fixed bed reactor in Run 99. In this run, since the zeolite/cobalt was diluted by the silica, eighteen rather than thirteen grams of catalyst were used. The amount of cobalt in the reactor in Runs 97 and 99 was thus the same. The bound catalyst was also evaluated in the slurry autoclave pilot plant in Run 61. Eighteen grams of catalyst were also used in this run, however, 290 grams of (C₃₀ oil) diluent were used. Since heat removal was expected to be much better in the slurry autoclave, the operating temperature was 221° C so that the performance data could be compared to that from Run 99 which operated at a *de-facto* temperature that was above the target inlet of 211° C. For Run 99 the catalyst was reduced at the normal temperature but *ex-situ* to the reactor. It was carefully transferred to the reactor under an inert atmosphere. The feed rate and operating pressure during the slurry autoclave run were the same as during Runs 97 and 99 (4.9 NL/hr·g Co and 287 psig, respectively). Performance data from Runs 97, 99 and 61 are compared in Figure 4.

After binding the catalyst was less active, possibly because the binder covered some of the catalyst active sites. Although the slurry autoclave was operated at a slightly higher temperature than the catalyst maximum temperature in Run 99, the conversions were similar in both runs. The methane selectivity during Run 61, however, was slightly lower than during Run 99. Unlike the screening runs in the fixed-bed reactor which were of short duration, Run 61 was four hundred hours long. During this run the conversions and selectivities appeared to approach a line out, however, some condition changes were made during the run making it difficult to absolutely judge the rate of catalyst deactivation. Additional slurry autoclave runs with high cobalt, Y zeolite-supported catalysts are needed.

Catalysts with levels of cobalt even higher than the Run 97 catalyst have been evaluated in the fixed-bed pilot under conditions identical to Run 97 except a lower level of catalyst was used. The results of these runs are summarized in Figure 5.

The catalyst loading used in Runs 110 and 123 is as low as practical. Obviously excess heat removal was still a problem at this low level. This means that increasing the cobalt level from eighteen to twenty-eight weight percent did result in the formation of quite a few additional active sites. The catalyst used in Run 110 contained ruthenium whereas the one used in Run 123 did not. Incorporation of small amounts of ruthenium into a cobalt catalyst composition should result in increased catalyst activity. This was not the case, however, the two very high cobalt catalysts above are merely first attempts. Perhaps the ruthenium is not yet well-dispersed into the cobalt. Modifications of the impregnation/activation procedures should be explored to see if additional activity can result from addition of ruthenium to the Y zeolite-supported catalyst composition. The catalyst bed maximum temperature was very high in Run 123, however, in spite of this the methane selectivity was not excessively high.

Apparently new active sites are formed as the level of cobalt on steamed, acid-washed Y zeolite is increased from 8 to 28 wt%. This is a significant observation because in LPFT processing the total volume of catalyst in the reactor will be critical. If a given volume of support can carry higher levels of catalytically active cobalt than previously thought possible, a superior LPFT catalyst will result. This is particularly true if these catalysts also retain the ability produce low levels of methane which, in fact, they do seem to do. Additional work with the very high cobalt-level catalysts is indicated. These should eventually be tested (after binding) in the slurry autoclave plant and compared to the catalyst evaluated in Run 61. However, before this additional compositions with small amounts of ruthenium should be prepared and screened in the fixed-bed plant. For LPFT processing catalyst activity is critical because of the low volume of catalyst that can be contained in an LPFT reactor, it is very important to find out if small amounts of ruthenium can activate the catalyst.

REFERENCES

1. H. Beuther, T. Kobylinski, C. Kibby and R. Pannell, U.S. Patent 4,585,798, 1986.
2. H. Beuther, C. Kibby, T. Kobylinski and R. Pannell, U.S. Patent 4,413,064, 1983.
3. H. Beuther, C. Kibby, T. Kobylinski and R. Pannell, U.S. Patent 4,493,905, 1985.
4. T. Kobylinski, C. Kibby, R. Pannell and E. Eddy, U.S. Patent 4,605,676, 1986.
5. R. Fiato, European Patent Application Publication No. 0 414 555 A1, filing date 8/23/90.

FIGURE 4**EVALUATION OF BOUND HIGH COBALT CATALYST:
FIXED-BED AND SLURRY AUTOCLAVE TESTING**

RUN NO.	LOADING CAT/DILUENT, g	MAX T °C	CO CONV, %	SELEC, MOL %		
				C ₁	C ₂	C ₂ "
97	13/160	222	72	13	1.8	0.1
99	13/160	216	55	12	2.1	0.1
61	13/290	221	58	10	1.9	0.1

FIGURE 5**HIGH VS. VERY HIGH COBALT LEVEL CATALYSTS**

RUN NO.	LOADING CAT/QUARTZ, g	MAX T °C	CO CONV %	SELEC, MOL%		
				C ₁	C ₂	C ₂ "
97	13/160	222	72	13	1.8	0.1
110	6.5/166.5	220	86	8.6	1.2	0
123	6.5/166.5	230	90	10.5	1.5	0

FIGURE 1

PROPERTIES: SUPPORTED OXIDES ON STEAMED Y ZEOLITE

CAT NO/RUN NO	SUPPORT SA ¹ /PV ²	METALS, WT%, AAS			
		Co	Mn	Zr	Ru
UNION CARBIDE/65	—	8.3	1.3	1.0	—
6827-81/97	582/0.56	17.6	2.0	1.6	1.0
6827-160/110	561/0.54	26.8	2.3	1.0	0.4
6827-161/123	588/0.55	28.7	1.8	1.1	—

1. m²/g
2. cc/g

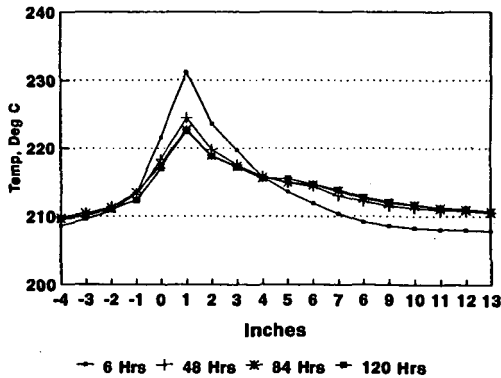
FIGURE 2

PERFORMANCE OF THE REFERENCE TO A HIGH COBALT CATALYST

RUN NO.	LOADING CAT/QUARTZ, g	MAX T °C	CO CONV, %	SELEC, MOL %		
				C ₁	C ₂	C ₂ '
65	13/160	213	40	7	0.6	0
97	13/160	222	72	13	1.8	0.1

FIGURE 3

CATALYST BED TEMPERATURE PROFILES DURING RUN 97



EFFECTS OF SUPPORTS AND PROMOTERS ON
COBALT F-T CATALYST BEHAVIOR IN FIXED BED
VS. SLURRY BUBBLE COLUMN REACTORS

R. Oukaci, J.G. Goodwin, Jr., G. Marcelin, and A. Singleton¹
Chemical & Petroleum Engineering Department
University of Pittsburgh
Pittsburgh, PA 15261

Keywords: Fischer-Tropsch Synthesis, CO Hydrogenation, Cobalt Catalysts.

INTRODUCTION

One of the most promising ways for producing liquid hydrocarbons from coal is via coal gasification to synthesis gas, followed by Fischer-Tropsch (F-T) synthesis to convert the syngas to a mixed product consisting mainly of straight chain hydrocarbons. Traditionally, iron catalysts have been used for F-T synthesis when the syngas is coal-derived, because they have the ability to simultaneously carry out the water gas shift reaction.

Recently, there has been renewed interest in the use of Co as a commercial F-T catalyst. Co has a higher specific activity than Fe (1,2); it produces primarily straight chain paraffins; and it has shown good lifetimes. The considerable commercial interest is evidenced by the large number of patents relating to Co catalysts and F-T processes which have been issued. These recently developed cobalt catalysts share some similarities in that they all consist of four major components: (a) the primary F-T metal, Co; (b) a second metal (Ru, Re, or other noble metal); (c) an oxide promoter (lanthana or zirconia, for example); and (d) a high surface area refractory oxide support (3).

Different types of reactor systems are proposed for commercial F-T synthesis. The slurry bubble column reactor has often been suggested as being one of the most appropriate for heat removal from the exothermic F-T synthesis reaction. However, most of the catalyst screening is carried out in fixed bed reactor systems, even for slurry bubble column reactor applications. In addition, there has been hardly any investigations of the effects of supports or promoters carried out in slurry bubble column reactor systems. Because of the different reaction conditions involved in these two systems, i.e., gas phase versus liquid phase, some of the effects observed in one system may not necessarily be found in the other.

A series of catalysts has been formulated in order to investigate the role of the supports and some promoters on affecting the F-T reaction both in a fixed-bed reactor as well as in a slurry bubble column reactor.

EXPERIMENTAL

All catalysts compared in this study consisted of 12-20 wt% cobalt, a second metal promoter (Ru or Re), and/or an oxide promoter such as zirconia, the support being alumina (Vista B), silica (Davison 952), or titania (Degussa P25).

¹ Energy International Corporation, 135 William Pitt Way, Pittsburgh, PA 15238.

These supports were chosen based on their low sulfur content and microspheroidal shape. The latter property is important when used in a slurry bubble column reactor as it prevents attrition.

All catalyst were prepared by impregnation of the supports with the appropriate solution of the nitrates of the various metals. After impregnation, the catalysts were dried at 120°C and calcined at temperatures no higher than 350°C. Prior to testing the catalysts were reduced in a flow of hydrogen. They have all been extensively characterized by different methods, including elemental analysis, BET physisorption, particle size distribution, X-ray diffraction, hydrogen chemisorption, temperature programmed reduction. Table 1 summarizes the relevant characterization data.

The catalysts were evaluated in terms of their activity and selectivity both in a fixed bed reactor and in a slurry bubble column reactor. Typically, 0.1 to 0.3 g of prerduced catalyst were charged into the tubular fixed-bed reactor and rereduced overnight at 300°C. The reaction was carried out at 220°C, 1 atm, H₂/CO ratio of 2.0, and a total flow rate of 50 cm³/min. No inert diluent was used. Sample analyses were taken after approximately 2, 5, 9, and 24 hours on-stream. In some cases the temperature was varied between 210° and 240°C in order to calculate an Arrhenius activation energy. Product analysis for C₁-C₂₀ hydrocarbons was performed by on-line gas chromatography. CO conversion rates were calculated based on the GC analysis of the products. Anderson-Schultz-Flory (A-S-F) distributions were plotted and the chain growth probability, α , calculated using the C₄-C₁₆ data.

For the slurry bubble column tests, the catalyst was first reduced *ex-situ* in a fluidized bed assembly and then transferred into a glove box for weighing and subsequent transfer into the slurry bubble column reactor. Approximately 15 g of catalyst and 200 g of liquid medium were used in a run. Typically, the reaction was carried out at 240°C, a total pressure of 450 psi, H₂/CO ratio of 2, and using 60% N₂ diluent. Analysis of the gas products, CO, CO₂, and C₁-C₅, was performed hourly. Liquid products were collected at the end of each 24 hour period, blended, and submitted for analysis. A-S-F plots of the liquid products were used to determine α . After reaching steady-state under these conditions, temperature, pressure, and H₂/CO ratio were varied in turn to study the effect of process conditions. A typical complete run lasted about 10 days.

RESULTS AND DISCUSSION

Table 2 shows selected data obtained from fixed bed reaction which indicate the effects of noble metal and ZrO₂ promotion and of the support on F-T activity and selectivity. The alumina- and silica-supported Co catalysts were found to be more active, by about a factor of two, than their titania- supported analog.

The addition of ruthenium to the γ -alumina supported cobalt catalyst increased its activity by a factor of ca. 6, while it had no effect on the silica-supported catalysts and only a slight enhancing effect on the activity of the TiO₂-supported catalyst. The effect on the Al₂O₃-supported catalyst may be explained by the fact that the presence of Ru increased the reducibility of the Co/Al₂O₃ catalyst while

it did not enhance the reducibility of the SiO₂ and the TiO₂-supported catalysts. In addition, hydrogen chemisorption measurements, shown in Table 1, show that the Ru promoter can increase the dispersion of the reduced Co/Al₂O₃. However, in the case of the SiO₂-supported catalyst, a factor of two in activity was gained by promotion with ZrO₂, although the latter did not seem to affect the reducibility of the cobalt or its dispersion.

It should be noted that neither the support nor the promoters changed significantly the characteristics of the reaction products, i.e., no significant change was noted in α or CH₄ formation rate. This suggests that the F-T reaction is still being carried out on Co sites and not on new sites created by the promoter. Similar results were obtained when Re was used as a metal promoter in place of Ru. The results obtained for Ru and Re promotion are similar to those reported in the patent literature (4-7).

Table 3 shows selected data obtained at 240°C, 450 psi, and H₂/CO ratio of 2, in the slurry bubble column reactor for Co/Al₂O₃ and Co/SiO₂ catalysts. In this case, the support was found to strongly influence the overall hydrocarbon production rate with little effect on α , while the addition of a noble metal promoter seemed to have little effect on the catalytic properties of cobalt. On the other hand, as in the case of the fixed bed testing, the ZrO₂ promoter was found to influence the overall activity of the silica-supported catalyst.

Obviously, diffusion limitations and gas solubilities in the liquid medium in the slurry bubble column reactor may play a role in some of the differences in the results from the two reaction systems. It is also possible that certain promoters or supports may function best in a narrow range of conditions. Clearly, ZrO₂ was the most consistent activity promoter.

ACKNOWLEDGMENTS

The authors gratefully acknowledge the funding of this project by DOE and the contribution of the following personnel involved in this study: S. Ali, L. Balawejder, P. Brim, B. Chen, W. Gall, G. Haddad, A. Kogelbauer, and S. Renaldi.

REFERENCES

- (1) M.A. Vannice, in *Catalysis: Science and Technology*, Vol. 3 (J.R. Anderson and M. Boudart, Ed.) Springer-Verlag, Berlin, 1982, pp. 139-198.
- (2) S.T. Sie, J. Eilers, and J.K. Minderhout, *Proc. Int. Cong. Catal.*, Calgary, 743 (1988).
- (3) J.G. Goodwin, Jr., Preprints of Div. of Petr. Chemistry, ACS Nat. Meeting, Atlanta, April 14-19, 1991. Pp. 156-159.
- (4) T.P. Kobylinski, C.L. Kibby, R.B. Pannell, and E.L. Eddy, *European Pt. Appl. O 253 924* (1986).
- (5) S. Erie, J.G. Goodwin, Jr., G. Marcelin, and T. Riis, U.S. Patent 4,801,573 (1989).
- (6) K.P. de Jong, J.H.E. Glazer, and M.F.M. Post, *European Pat. Appl. O 221598* (1986).
- (7) C.H. Mauldin, U.S. Pat. 4,568,663 (1986).

Table 1. Catalyst Characterization Results.

CATALYST	COMPOSITION		BET Surface Area (m ² /g cat)	H ₂ CHEMISORPTION			H ₂ IPR % Red. 25-900°C	XRD Co ₃ O ₄ d _p (nm)
	Co (wt%)	Promoter (wt%)		Total H ₂ (μmol/g cat)	d _p ¹ (nm)	Co Disp. ² (%)		
Co/Al ₂ O ₃	20	0	173	48	21	2.8	85	20
RuCo/Al ₂ O ₃	20	Ru 0.5	158	185	9	11	97	23
Co/SiO ₂	20	0	211	89	15	5	80	24
RuCo/SiO ₂	20	Ru 0.5	-	112	-	7	-	-
ZrCo/SiO ₂	20	Zr 8.5	208	93	-	5	75	-
ZrRuCo/SiO ₂	20	Zr 8.5 Ru 0.5	214	70	-	4	-	-
Co/TiO ₂	12	0	13	19	40	2	72	38
ReCo/TiO ₂	12	Re 0.8	16	44	19	4	80	39
RuCo/TiO ₂	12	Ru 0.5	15	38	21	4	79	45

(1) Average particle diameter based on the reduced cobalt.

(2) Co dispersion based on the total cobalt.

Table 2. Fixed Bed Reaction Data

CATALYST	RATE		SELECTIVITY	
	(g CH ₂ /g cat/hr)	mol CO/mol Co/s x 10 ⁻⁴	CH ₄ (wt%)	α
Co/Al ₂ O ₃	0.073	4.3	29.2	0.62
RuCo/Al ₂ O ₃	0.470	28.0	29.0	0.60
Co/SiO ₂	0.083	4.8	28.9	0.65
RuCo/SiO ₂	0.085	4.9	18.9	0.73
ZrCo/SiO ₂	0.160	9.4	23.5	0.63
RuZrCo/SiO ₂	0.136	8.0	-	0.69
Co/TiO ₂	0.021	2.0	-	0.64
ReCo/TiO ₂	0.052	5.1	45.0	0.49
RuCo/TiO ₂	0.034	3.3	27.7	0.69

P = 1 atm, T = 220°C, H₂/CO = 2, Conversion < 5%, Time-on-stream = ca. 25 hrs

Table 3. Slurry Bubble Column Reaction Data

CATALYST	RATE (g CH ₂ /g cat/hr)	SELECTIVITY	
		CH ₄ (wt%)	α
Co/Al ₂ O ₃	1.34	7.9	0.82
RuCo/Al ₂ O ₃	1.57	9.7	0.85
Co/SiO ₂	0.63	6.1	0.89
RuCo/SiO ₂	0.66	-	0.86
ZrCo/SiO ₂	1.24	10.7	0.82
RuZrCo/SiO ₂	1.16	11.0	0.85
Co/TiO ₂	0.09	-	-
ReCo/TiO ₂	0.13	0.1	0.85
RuCo/TiO ₂	0.40	8.3	0.83

Catalyst weight: ca. 15g; T = 240°C; P = 450 psi; H₂/CO ratio = 2; total flow rate: ca. 15 L/min, or 3 cm/sec linear velocity; diluent: ca. 60% N₂.

ATTRITION AND CARBON FORMATION ON IRON CATALYSTS

Steven D. Kohler, Mark S. Harrington, and Nancy B. Jackson
Sandia National Laboratories
P.O. Box 5800, MS 0790
Albuquerque, NM, 87185-0790

KEYWORDS: Attrition, carbon deposition, slurry bubble column

ABSTRACT

A serious engineering problem that needs to be addressed in the scale-up of slurry-phase, Fischer-Tropsch reactors is attrition of the precipitated iron catalyst. Attrition, which can break down the catalyst into particles too small to filter, results from both mechanical and chemical forces. This study examines the chemical causes of attrition in iron catalysts. A bench-scale, slurry-phase CSTR is used to simulate operating conditions that lead to attrition of the catalyst. The average particle size and size distribution of the catalyst samples are used to determine the effect of slurry temperature, reducing gas, gas flow rate and time upon attrition of the catalyst. Carbon deposition, a possible contributing factor to attrition, has been examined using gravimetric analysis and TEM. Conditions affecting the rate of carbon deposition have been compared to those leading to attrition of the precipitated iron catalyst.

INTRODUCTION

In the investigation of the use of slurry-phase bubble columns for exothermic synthesis gas reactions, including Fischer-Tropsch synthesis and methanol synthesis, one of the biggest challenges presented by the process is development of the catalyst. In the typical Fischer-Tropsch use of the bubble column, the catalyst is suspended in a wax and synthesis gas is bubbled up through the column. Since the Fischer-Tropsch process produces wax, the wax must be continuously extracted from the column and the catalyst must be separated from the wax for sake of purity and to keep the catalyst concentration constant within the reactor. Therefore, the catalyst must be large enough to be filtered easily from the wax, but as small as feasibly possible to enhance activity. Catalyst attrition is a major problem at low H_2/CO ratios with carbon deposition proposed as the contributing factor to chemical attrition of the catalyst.

EXPERIMENTAL

The catalyst used in this study was a precipitated and spray-dried, proprietary iron catalyst made by United Catalyst Inc. for the U.S. Department of Energy. The catalyst consisted of iron oxide and copper oxide in a ratio of about 9:1. Trace amounts of potassium oxide were also present. Transmission electron microscopy (TEM) and scanning electron microscopy (SEM) of the untreated catalyst particles showed that the samples were about 20-50 μm in diameter with a significant amount of micron and submicron fines. The larger particles were made up of angular, faceted, single-crystal grains (1-2 μm) with similar orientation that were agglomerated together. See Figure 1. The particle size of three similarly prepared Fischer-Tropsch catalysts were measured using a sedimentation-type particle size analyzer. Particle size analysis confirmed the existence of large amounts of micron and submicron fine particles. Particle size measurements are listed in Table 1.

The transmission electron microscopy was performed on a 200 kV JEOL JEM 2000FX microscope and the scanning electron microscopy utilized a Hitachi S800 microscope. Thermal gravimetric analysis (TGA) was performed using a Dupont 951 Thermalgravimetric Analyzer.

Carbon deposition was studied during pretreatment and during Fischer-Tropsch synthesis by TGA and TEM. The catalysts were pretreated in the TGA or in a microreactor for TEM work with H_2 or CO at 270°C and then reacted in H_2/CO (0.7:1) at 250°C, 275°C, and 300°C. The catalysts were pretreated for 10-14 hrs and reacted for 10-14 hrs in the TGA. In the microreactor for TEM studies, the catalysts were pretreated for 3 hrs and reacted for 3 hrs.

RESULTS

Analysis in TEM showed that activation in carbon monoxide before reaction in synthesis gas deposited more carbon on the surface of the catalyst than activation in hydrogen before reaction. The deposited carbon was amorphous in structure. All catalysts, regardless of pretreatment, appeared to have both carbide and oxide phases present after reaction. As the temperature of the synthesis gas reaction is increased, the thickness of the carbon deposited on the iron oxide

catalyst also increased. Pretreatment in CO followed by synthesis gas at 300°C showed the thickest layer of amorphous carbon. The individual grains showed signs of separation; the agglomerate was breaking up. The diffraction pattern showed a greatly diminished oxide phase while the pattern of the carbide phase suggested randomly oriented grains with loss of orientation relative to the original crystal. This breakup was also seen in catalysts pretreated in hydrogen and followed by synthesis gas at 300°C. It also appears from TEM that there is a breakdown of the parent agglomerate template at synthesis temperature greater than 275°C which causes separation of the catalyst into individual crystallites (1-2 μm in size) which leads to attrition over time. At synthesis temperatures below 275°C, oxidation of the iron catalyst showed a return of the original microstructure of the catalyst. Oxidation immediately following pretreatment of the catalyst in either H₂ or CO caused a return to the original microstructure.

TGA results confirm the increase in the amount of amorphous carbon during pretreatment in carbon monoxide and at higher synthesis reaction temperatures. In addition, TGA results indicate that the breakdown of the catalyst due to carbon deposition can occur at temperatures lower than 275°C, but at reaction times longer than those analyzed using TEM. TGA results show that regardless of the temperature of reaction or pretreatment gas, as the reaction in synthesis gas proceeds, the catalyst continues to gain weight at a rate proportional to the temperature. This continued weight gain implies continued carbon deposition leading to an eventual breakdown of the catalyst agglomerate into individual particles. The weight gain of the samples in the TGA due to synthesis reaction is shown in Table 2.

CONCLUSIONS

1. TEM analyses show that at reaction temperatures above 275°C there is significant carbon deposition and a breakdown of the parent iron catalyst agglomerate which causes the particles to disintegrate into individual crystallites (1-2 μm in size), a phenomena which would lead to attrition.
2. Pretreatment in CO followed by synthesis gas at 300°C showed the thickest layer of amorphous carbon in TEM.
3. The amount of carbon deposited increased with increasing temperature. The deposition rate was proportional to temperature.
4. TGA results show that weight gain continues at reaction temperatures below 275°C. The continued weight gain implies continued carbon deposition which could lead to eventual breakdown of the agglomerate into individual crystallites.
5. The diffraction pattern of the catalyst after reaction showed both a carbide and oxide phase. The diffraction pattern did not depend upon the pretreatment gas used.

ACKNOWLEDGMENTS

The authors would like to thank Dr. Abhaya Datye and his students, Dinesh Kalakkad and Mehul Shroff, of the University of New Mexico for the TEM and SEM work. This work performed at Sandia National Laboratories, which is funded by the U.S. Department of Energy under contract DE-AC04-94AL85000.

SAMPLE	NUMBER DISTRIBUTION MEDIAN DIAMETER	NUMBER DISTRIBUTION MODAL DIAMETER	MASS DISTRIBUTION MEDIAN DIAMETER	MASS DISTRIBUTION MODAL DIAMETER
CATALYST A	0.37 μm	0.31 μm	7.97 μm	28.85 μm
CATALYST B	0.32 μm	0.20 μm	22.22 μm	30.93 μm
CATALYST C	NOT AVAILABLE	10.0 μm	10.24 μm	21.94 μm

Table 1 - Particle size analysis of iron oxide catalysts

PRETREATMENT GAS	PRETREATMENT TEMPERATURE 250°C	PRETREATMENT TEMPERATURE 275°C	PRETREATMENT TEMPERATURE 300°C
HYDROGEN	0.045 mg/hr	0.083 mg/hr	0.11 mg/hr
CARBON MONOXIDE	0.22 mg/hr	0.68 mg/hr	1.84 mg/hr

Table 2 - Rate of catalyst weight gain during reaction in synthesis gas at 270°C. Weight gain was measured by thermal gravimetric analysis after pretreatment in either hydrogen or carbon monoxide at 250°C, 275°C, or 300°C.

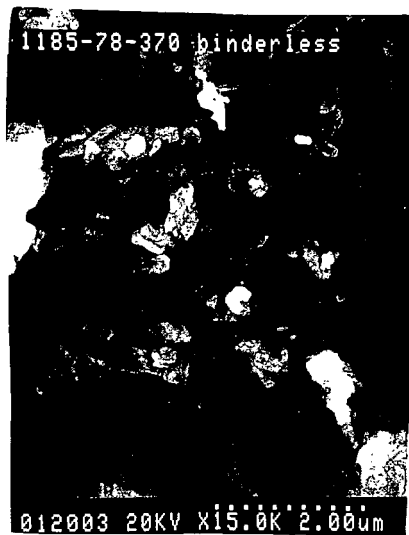


Figure 1 - SEM shows that the surface of the iron catalyst consists of agglomerated smaller, angular crystallites, which are particularly susceptible to attrition.

FIGURE 1

PROPERTIES: SUPPORTED OXIDES ON STEAMED Y ZEOLITE

CAT NO/RUN NO	SUPPORT SA/PV ²	METALS, WT%, AAS			
		Co	Mn	Zr	Ru
UNION CARBIDE/65	—	8.3	1.3	1.0	—
6827-81/97	582/0.56	17.6	2.0	1.6	1.0
6827-160/110	561/0.54	26.8	2.3	1.0	0.4
6827-161/123	588/0.55	28.7	1.8	1.1	—

1. m²/g
2. cc/g

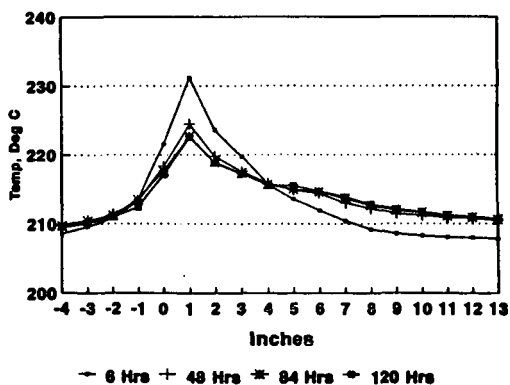
FIGURE 2

PERFORMANCE OF THE REFERENCE TO A HIGH COBALT CATALYST

RUN NO.	LOADING CAT/QUARTZ, g	MAX T °C	CO CONV, %	SELEC, MOL %		
				C ₁	C ₂	C ₂ ⁺
65	13/160	213	40	7	0.6	0
97	13/160	222	72	13	1.8	0.1

FIGURE 3

CATALYST BED TEMPERATURE PROFILES DURING RUN 97



ULTRAFINE PARTICLES OF IRON IN FISCHER-TROPSCH SYNTHESIS

Devinder Mahajan and Kaumudi Pandya
Department of Applied Science, Building 815
Brookhaven National Laboratory
Upton, NY 11973-5000

Keywords: Fischer-Tropsch, Catalysis, Ultrafine Particles

INTRODUCTION

Though direct combustion of natural gas is the most efficient use of this abundant, inexpensive, and cleaner fossil fuel, its potential to replace existing less efficient feedstocks for downstream processes is enormous. Direct conversion of methane to useful products under mild conditions is an ongoing area of research, and a few reported successes include higher hydrocarbons (C_2 - C_6) synthesis on Pt at 250°C,¹ Hg-catalyzed synthesis of methanol at 180°C,² and acetic acid synthesis catalyzed by aqueous $RhCl_3$ at 100°C.³ Since these approaches are in early stages of development, improvements in other known routes are of interest. Fischer-Tropsch (F-T) synthesis is an indirect route to catalytic production of liquid fuels from synthesis gas derived from carbonaceous sources. The process is still uneconomical for widespread use due to low space-time-yield (STY), low product selectivity, and catalyst intolerance to sulfur. To address these aspects, a few reports⁴ describe the use of ultrafine particle (UFP) catalysts in slurry-phase F-T synthesis. We recently reported⁵ that a commercially available unsupported UFP Fe_2O_3 material (NANOCAT™) (Mean particle diameter (MPD) = 3 nm; surface area (SA) = 255 m²/g) slurried in a C_{30} hydrocarbon solvent, after reduction at 280°C under CO, catalyzed conversion of balanced synthesis gas ($H_2/CO = 2/1$) at $\geq 220^\circ C$ and ≤ 3 MPa. Described below are additional runs carried out to further scrutinize the Fe UFP system.

EXPERIMENTAL

Unit Description

All runs were carried out in a continuous gas flow unit customized to handle F-T synthesis. The core of the unit was a 1L stirred reactor rated at 40 MPa at 343°C commercially available from Autoclave Engineers (AE). The unit was fitted with a mass flow meter to measure in-flow gas. Before entering the reactor, gas was purified by passing through Scott charcoal and molecular sieve filters. On the reactor head, several gas/liquid ports were provided to allow: 1) inlet gas through a dip tube, 2) catalyst sampling during a run, 3) liquid removal through a 0.5 μ filter to avoid catalyst loss. Unreacted gas and volatile products exited the reactor and passed through a heated line to a 0.5 L hoke bomb, maintained at ambient temperature, where almost all of water and higher hydrocarbons condensed. The remaining gas passed through two 1L and 2L tanks maintained at 5°C and -45°C respectively. The dry gas was vented in a fume hood after passing through a dry test meter.

Analysis

Gases (H_2 , CO, CO_2) were analyzed in the TCD mode under an argon flow on a Gow Mac 580 gas chromatograph fitted with a Poropak R column. Gaseous and liquid hydrocarbons were analyzed in the FID mode under a helium flow on a Perkin Elmer 8500 gas chromatograph fitted with an alumina column, whereas oxygenates in aqueous phase were analyzed in the TCD mode on a Poropak Q column.

Materials

Samples of NANOCAT™ (α -Fe₂O₃; mean particle diameter (MPD) = 3 nm; surface area (SA) = 255 m²/g; d (bulk) = 0.05 g/mL), from MACH-1, Inc., Ethylflopolyolefin-164 solvent, a dec-1-ene homopolymer (composition: 84.4% trimer, 14.5% tetramer; b.pt. = 518°C; d = 0.818 g/mL; mol. wt. = 437) from Ethyl Corporation, and UCI catalyst (Fe₂O₃ = 69.6, K₂O = 5.1, SiO₂ = 8.3, CuO = 2.6, loss on ignition (LOI) = 14.8, all in wt%; MPD = 32.5 μ m; SA = 232 m²/g from Air Products and Chemicals, Inc. were obtained. Gases were purchased from Scott Specialty Gases.

Catalyst Reduction

A 4.6 wt% NANOCAT™ in 330 g ethylflopolyolefin-164 solvent was loaded under argon into the 1L AE reactor. The vessel was flushed twice with 0.6 MPa CO before pressurizing to 1.43 MPa. The slurry temperature was slowly raised to 280°C under a 0.2 L/min CO flow. The CO₂ concentration in the exit gas maximized to 4.3 vol% in 5 hours and then decreased to 0.3 vol% at 24 hours. At this time, the catalyst was assumed to be > 95% carbided. A similar CO₂ evolution profile was obtained with the UCI catalyst except that the CO₂ maximum was attained in about 2 hours. A freshly reduced catalyst was used in each run.

F-T Synthesis

After catalyst reduction, the temperature was lowered to a desired value, CO replaced with preblended syngas, and the reactor maintained at a set pressure. Typical reaction conditions were: P = 2.77 MPa; syngas: H₂/CO = 65%/35%; gas hourly space velocity (GHSV) = 5.45-5.75 normal liters (NL).g Fe⁻¹.h⁻¹; stirring speed = 250 rpm.

RESULTS AND DISCUSSION

NANOCAT™, an unsupported Fe UFP catalyst with MPD of 3 nm, was of interest in this study. Though this was identified as α -Fe₂O₃ by the manufacturer, a recent EXAFS/XANES study⁶ described this material to be iron oxyhydroxide (FeOOH·xH₂O) with surface iron ions having tetrahedral symmetry and water molecules adsorbed on the surface. For data comparison, the UCI catalyst was selected. This supported material contained about 11,000 times larger particles (MPD = 32.5 μ m) of α -Fe₂O₃. For the F-T reaction described here, a low (4.6 wt%) catalyst loading was selected to avoid mass transfer problems at low gas feed rates used. The precursor materials were initially reduced with CO at 280°C to generate the iron carbide phase.⁷ A time profile of CO₂ in the exit gas indicated that reduction beyond 24 hours was unnecessary. Since nature of the pretreatment has a profound effect on catalyst performance,⁷ the same reduction procedure was used in all the runs.

Since the commercial F-T synthesis is carried out at T > 260°C,⁷ performance of the subject catalysts was initially evaluated at 260°C. After the F-T reaction was initiated, CO and H₂ conversions quickly maximized at 91 and 62% respectively. These values dropped to 61 and 52% at 50 hours and then slowly to 44 and 43% at 200 hours. Two subsequent runs at 240° and 220°C showed similar behavior. At 240°C, CO and H₂ conversions were 89, 35, 35% and 62, 38, 32% at 1, 50, 120 hours. At 220°C, the values were 61, 37, 36% and 49, 27, 25% at 5, 50, 200 hours respectively. Since no non-volatile liquid was drained from the reactor during these runs, a decrease in conversion values observed during steady-state (50-200 h) can be attributed to a steady increase in the liquid volume though any contribution from catalyst deactivation cannot be ruled out. The corresponding H₂/CO consumption ratio increased for runs at 260°C

(1.26 (1 h) to 1.81 (200 h)) and 240°C (1.40 (1 h) to 1.87 (120 h)) with time but decreased from 1.45 (5 h) to 1.22 (200 h) at 220°C.

In Table 1, volumetric yield of hydrocarbons produced and CO conversion values are compared as a function of temperature. Though CO conversion increased with Fe UFP with temperature (37.1 and 54.6% at 220 and 260°C respectively), this change was more dramatic with the UCI reference catalyst where the corresponding values changed from 7 to 68.8%. But as shown in Figure 1, any temperature-related increase in CO consumption translated into concomitant increase in hydrocarbons as well as CO₂ concentrations. With Fe UFP, a 17.5% increase in CO consumption shifted the overall product selectivity by a 30.7 wt% decrease in hydrocarbons but a 30.8 wt% increase in CO₂ (Figure 1). With UCI, a 61.8% increase in CO consumption (Table 1) resulted in product selectivity of hydrocarbons and CO₂ changing from 34.3 to 28.8 wt% and 20.3 to 46 wt% respectively. The volumetric yield values showed about 50% increase for Fe UFP but a factor of three for UCI both for C₁-C₄ and C₅₊ products (Table 1).

The effect of temperature on hydrocarbon distribution resulting from Fe UFP catalyzed F-T reaction is shown in Table 2. The C₁₁₊ fraction decreased with temperature whereas the C₅-C₁₀ and C₂-C₄ fractions showed an increase. CH₄ increased from 10.5 to 17.3 wt% at 220 to 240°C but then decreased to 15.9 wt% at 260°C.

The hydrocarbon product distribution data were used to yield Schulz-Flory plots and α (probability of hydrocarbon chain growth) was calculated from the slope. The α values were 0.56, 0.57, 0.65 (Fe UFP) and 0.53, 0.58, 0.64 (UCI) at 220, 240, 260°C.

In Figure 1, as plotted, the aqueous phase values included oxygenates (5.7, 10.1, 6.0 wt% at 220, 240, 260°C). Also, as already reported,⁵ the CO₂ data at 220°C are of interest. During this run, the total CO₂ generated decreased from a high of 23.9% (at 7 h) to 1.44% in 120 hours. Thereafter, no CO₂ was detected in the product stream suggesting no water-gas-shift (WGS) activity. Incidentally, WGS activity could be restored by raising the temperature. A recent⁸ technology review of slurry-phase F-T synthesis with CO-rich synthesis gas suggests the following equation to calculate temperature (T,K) dependence of the equilibrium constant (K_{eq}) for the WGS reaction:

$$K_{eq} = 0.0132 \exp(4578/T) \quad (1)$$

From the presented data of the Fe UFP and UCI systems, some preliminary conclusions are noteworthy. Since the unsupported UFP system permitted a higher iron loading, volumetric efficiency was higher with this system but showed a less dramatic decrease with decreasing temperature. The 220°C data of Fe UFP is of particular interest because the absence of WGS activity was demonstrated with balanced gas. Moreover, the Fe UFP system appeared more stable at 220°C since CO conversion declined less sharply (37 to 36%) compared to that at 260°C (61 to 44%) in 150 hours. Since particle aggregation is a function of temperature,⁷ this phenomenon may explain an overall better performance exhibited by Fe UFP at lower temperatures. EXAFS and Mössbauer data of the final Fe UFP catalyst from the 260°C run showed iron to be in the magnetite phase. Similar and other relevant studies are presently being carried out on these systems and will be the subject of a forthcoming publication.⁹

ACKNOWLEDGEMENT

The authors thank the US Department of Energy (under Contract No. DE-AC02-76CH00016) for financial support through the Pittsburgh Energy Technology Center (PETC).

REFERENCES

1. M. Belgued, P. Parja, A. Amariglio, and H. Amariglio. *Nature* **352** 789-90 (1991).
2. R. A. Periana, D. J. Taube, E. R. Evitt, D. G. Löffler, P. R. Wentrcek, G. Voss, and T. Masuda. *Science* **259** 340-3 (1993).
3. M. Lin and A. Sen. *Nature* **368** 613-5 (1994).
4. E. Kikuchi and H. Itoh, in *Methane Conversion*, ed. D. M. Bibby, C. D. Chang, R. F. Howe, and S. Yurchak, Elsevier Science Publishers B.V., Amsterdam, The Netherlands, 1988, 517; H. Itoh and E. Kikuchi. *Appl. Catal.* **67** 1 (1990).
5. D. Mahajan, A. Kobayashi, and N. Gupta. *J. Chem. Soc. Chem. Commun.* 795-6 (1994).
6. J. Zhao, F. E. Huggins, Z. Feng, F. Lu, N. Shah, and G. P. Huffman. *J. Catal.* **143** 499-509 (1993).
7. M. E. Dry, in *CATALYSIS - Science and Technology*, ed. J. R. Anderson and M. Boudart, Springer-Verlag, Berlin, Heidelberg, 1981, vol. 1, chapter 4.
8. V. U. S. Rao, G. J. Stiegel, G. J. Cinquegrane, and R. D. Srivastava. *Fuel Process. Tech.* **30** 83-107 (1992).
9. D. Mahajan, A. Kobayashi, and K. Pandya. Manuscript in preparation.

Table 1. Volumetric yields and CO conversion as a function of temperature during Fe UFP^a and UCI^a catalyzed F-T synthesis.^b

T, °C	220	240 ^c	260
<u>Fe UFP</u>			
CO conversion, %	37.1	40.8	54.6
Volumetric yield, kg.Lcat ⁻¹ .h ⁻¹			
C ₁ -C ₄	0.008	0.009	0.012
C ₅₊	0.004	0.005	0.006
<u>UCI</u>			
CO conversion, %	7.0	27.0	68.8
Volumetric yield, kg.Lcat ⁻¹ .h ⁻¹			
C ₁ -C ₄	0.003	0.005	0.008
C ₅₊	0.002	0.004	0.006

^aCatalysts were prerduced under 1.43 MPa CO at 280°C for 24 h.

^bTypical F-T conditions were: 4.6 wt% catalyst slurried in 330 g ethylflopolyolefin-164; P = 2.77 MPa; syngas: 65% H₂/35% CO; stirring speed = 250 rpm; space velocity = 5.45-5.75 NL.gFe.⁻¹h⁻¹. On-line time = 200 h.

^cOn-line time = 120 h.

Table 2. Hydrocarbon product distribution^a as a function of temperature during F-T synthesis^b catalyzed by Fe UFP.

T, °C	220	240	260
C ₁	10.5	17.3	15.9
C ₂ -C ₄	32.0	35.4	38.0
C ₅ -C ₁₀	24.1	28.3	30.1
C ₁₁ +	33.4	19.0	16.0

^aIn wt%.

^bRun conditions same as in the footnotes of Table 1. Data at 120 hours.

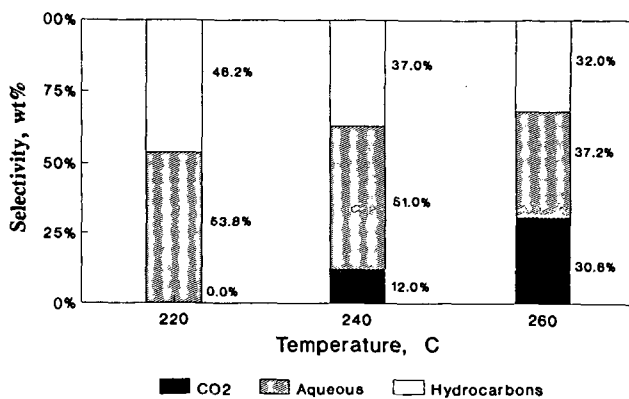


Figure 1. Total product selectivity as a function of temperature. Value shown were at 120 h. The aqueous phase also contained some oxygenates. Reaction conditions were the same as in footnotes of Table 1.

ISOBUTYLENE SYNTHESIS FROM HYDROGEN LEAN SYNGAS IN SLURRY AND TRICKLE BED REACTORS

Can Erkey, Rayford G. Anthony and Aydin Akgerman
Chemical Engineering Department
Texas A&M University
College Station, TX 77843-3122

Keywords: Isobutylene, syngas, multiphase reactors

INTRODUCTION

Due to environmental regulations, new gasoline formulations will be introduced to the market in the coming decade to reduce automobile exhaust emissions of CO, nitrous oxides and photoreactive unburned hydrocarbons. Addition of oxygenates such as methyl tertiary butyl ether (MTBE) to new formulations is necessary to maintain an acceptable octane number required for modern automobiles. The production of MTBE is currently limited by the supply of isobutylene. We and other groups have recently reported data on selective formation of isobutylene from hydrogen lean synthesis gas (isosynthesis) in fixed beds over catalysts based on zirconia in the temperature range 573-723 K and the pressure range 0.5 - 100 atm. All the studies in the literature on isosynthesis have been conducted in gas-solid fixed bed reactors. Using a three phase gas-oil-catalyst slurry or trickle bed reactor for isosynthesis can have certain advantages. Continuous circulation of the oil phase may enable separation of light components from the heavy components (C_3+ which are produced by the reaction) at the gas oil separator. The heavy components can be circulated back to the reactor dissolved in the oil and further converted into light hydrocarbons. The CO/H_2 ratio in the oil phase may also be quite different than the CO/H_2 ratio in the feed gas due to the differences in Henry's Law Constants for hydrogen and carbon monoxide which may affect the product distribution. The reaction can be run in the absence of mass transfer limitations in a slurry reactor. There is evidence in the literature that isosynthesis reactions become controlled by external mass transfer at temperatures above 723 K. Other advantages for the slurry reactor include better temperature control and low capital costs, as opposed to fixed bed reactors. In this study, we report the results of experiments on isosynthesis conducted in a laboratory scale slurry reactor and a trickle bed reactor.

EXPERIMENTAL

A schematic diagram of the trickle bed and slurry reactor system is shown in Figure 1. The feed gases are purified by flow through a guard bed consisting of activated carbon and molecular sieves with particle size of 0.16 cm. Hydrogen and carbon monoxide flowrates are controlled with Brooks model 5850E mass flow meters which have flow ranges of 0-2 and 0-1.5 standard liters per hour, respectively. The flow meters were calibrated by checking the controller set point versus the volumetric flowrate determined by the bubble meter. The feed gas streams are combined at a predetermined CO/H_2 ratio. To enhance mixing, the gases are passed through a bed of glass beads prior to the reactor. Decalin was fed to the unit using a Milton Roy pump. A relief valve, which is set at 106 atm, was placed before the reactor to prevent uncontrolled pressure rises in the system.

The trickle bed reactor is a 316 stainless steel tube, 25 cm long, 0.96 cm ID, and 1.2 cm OD. It was mounted vertically in a bed of aluminum pellets. The reactor is divided into three sections. Prior to and after the 7 cm catalyst bed are 6 and 12 cm supporting sections filled with 0.2 cm diameter glass beads. The reactor was heated by the heating block and controlled by a Omega model 6100 temperature controller. A thermocouple inserted through the middle of the catalyst bed was used to measure the temperature of the bed.

The slurry reactor was a stirred 100 cm³ Autoclave model EZ seal with six ports and one thermowell. The feed was introduced to the bottom of the reactor through a dip tube. A 50 micron porous metal filter was connected to the effluent port to prevent the entrainment of catalyst particles. A baffle bar and impeller were connected to the stainless steel reactor cover. The impeller was driven by a Magnadrive II stirrer. Cooling water was passed through the Magnadrive assembly to keep the temperature of the assembly in the permissible range. The reactor was heated using a furnace supplied by the manufacturer which was controlled by a Thermolyne Furnatrol I furnace controller.

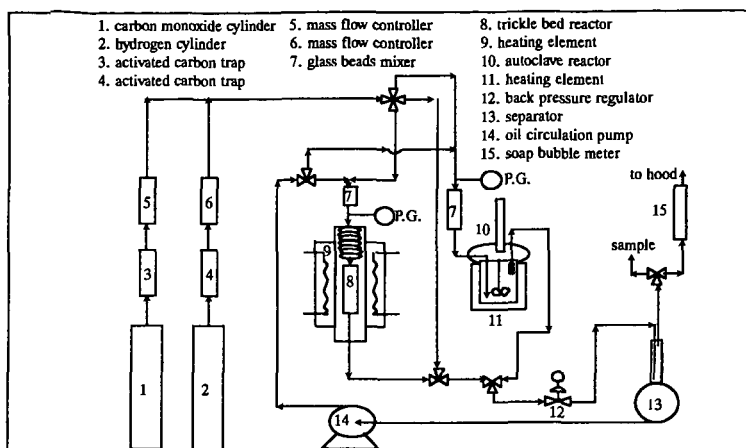


Figure 1. Schematic diagram of the experimental set-up

The reactor pressure was maintained with a Grove model 91W back pressure regulator. The reactor effluent passed through the back pressure regulator where the pressure was reduced to atmospheric pressure prior to the gas oil separator. The decalin collected at the bottom of the separator was recycled to the reactor. After the gas oil separator a sampling port was used to take gas samples for analysis. The effluent gas was passed through a soap bubble meter to measure the volumetric flow rate before it was vented to a fume hood. The decalin used in this study was obtained from Sigma Chemical and exists as *cis* and *trans* isomers of decahydronaphthalene with a minimum purity of 98 % as determined by gas chromatography.

RESULTS AND DISCUSSION

Slurry reactor

Zirconia was synthesized in the laboratory by precipitation. It had a surface area of 92 m²/g. Figure 2 shows a comparison of the hydrocarbon product distributions for the slurry and fixed bed reactors. The comparisons have been made at similar space velocities and similar conversions. Although the CO conversion is lower for the slurry reactor at a fixed space velocity, the selectivities to light hydrocarbon products are higher at equal conversions, and less C₅+ products are produced. This is due the fact that some of the heavier C₅+ products formed during the reaction are circulated back to the reactor in the oil and further crack to lighter hydrocarbons. The lower CO conversion for the slurry reactor at equal space velocity can be entirely accounted by lower performance of a CSTR as opposed to a PFR. As seen in Figure 3, changes were observed in the distribution of C₄ products. Figure 4 shows the comparison of product distribution for different CO/H₂ ratios.

The mass transfer resistances were calculated based on the data. Gas bubble to liquid mass transfer coefficients were calculated using the Calderbank and Moo-Young correlation and liquid to particle mass transfer coefficients were calculated using various correlations in the literature. These resistances were found to be negligible. The effectiveness factors were found to be very close to unity. Therefore, it is believed that the reactions were run in the kinetically controlled regime in the absence of any mass transfer limitations.

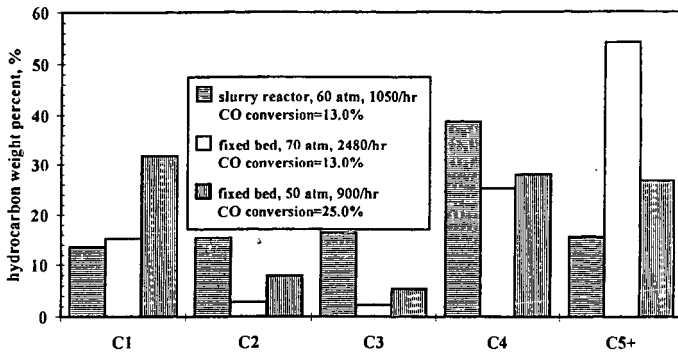


Figure 2. Hydrocarbon product distributions in fixed bed and slurry reactors at 400 °C.

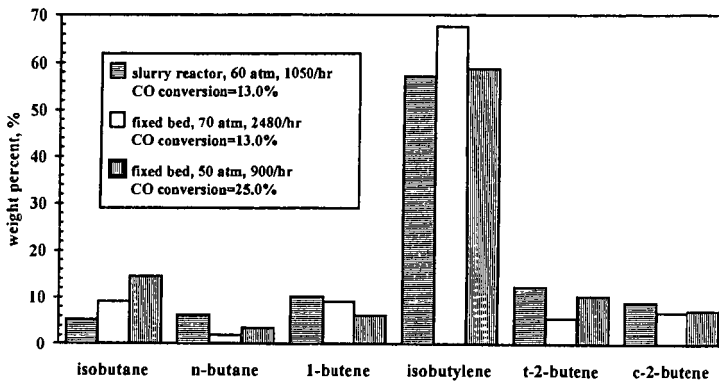


Figure 3. C₄+ product distributions in fixed bed and slurry reactors at 400 °C.

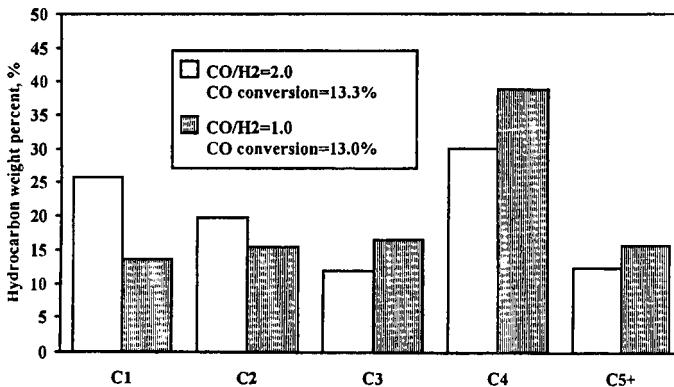


Figure 4. Effect of CO/H₂ ratio on hydrocarbon product distribution at 400 °C.

Trickle bed reactor:

Experiments using the trickle bed reactor were conducted with commercial zirconia with a surface area of 52 m²/g. A comparison of the performance of the catalyst when operating the reactor in the fixed and trickle bed modes at 669 K and 51 atm is shown in Figures 5 and 6. The selectivity for isobutylene and the C₄ components was higher when operating the reactor as a conventional gas phase fixed bed reactor than when operating the reactor as a trickle bed. The CO conversion was approximately the same for both modes of operation. The product distribution obtained with the trickle bed contains more C₃'s, C₄'s and methane and less C₅+ than the product distribution obtained when operating in the gas phase fixed bed reactor mode. A greater amount of propylene is produced in the trickle bed than with the fixed bed gas phase reactor. As shown in Figure 7, oil flow rates were shown to have minor effects on the product distribution. Figure 8 shows that as oil flow rate increases, a slight decrease in CO conversion is observed. This may be due to the decrease of the residence time of the gas through the reactor.

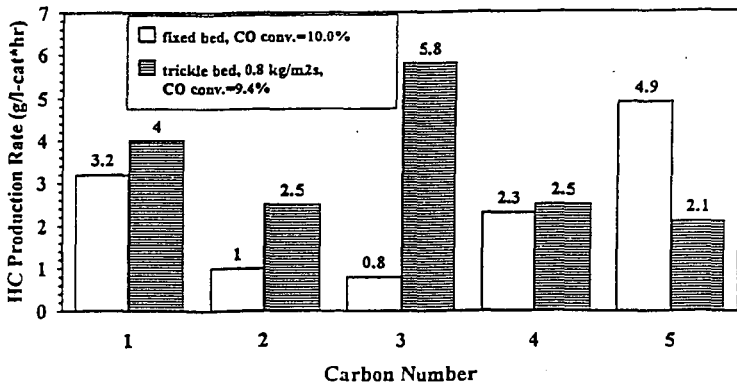


Figure 5. Comparison of hydrocarbon product distribution for fixed and trickle bed reactors at 669 K, 51 atm, 1/1 CO/H₂ ratio and 89 seconds space time.

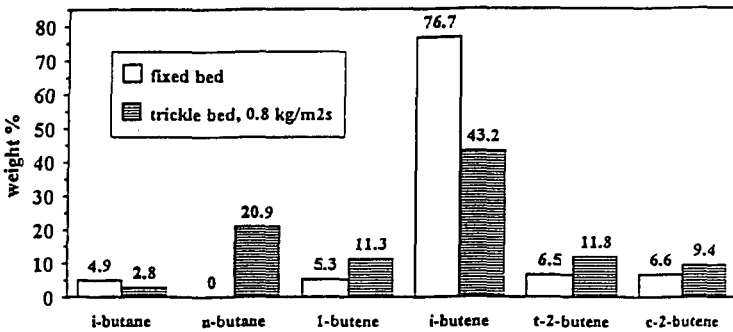


Figure 6. Comparison of C₄ distribution for fixed and trickle bed reactors at 669 K, 51 atm, 1/1 CO/H₂ ratio and 89 seconds space time.

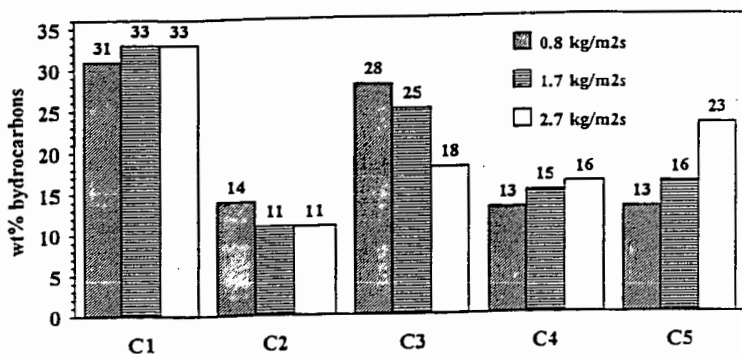


Figure 7. Change in hydrocarbon distribution with oil flowrate at 669 K, 51 atm, 1/1 CO/H₂ ratio and 668 (1/hr) space velocity.

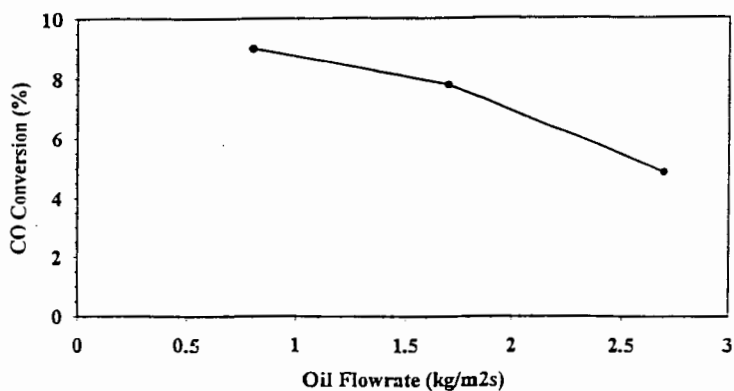


Figure 8. Variation of CO conversion with oil flow rate in the trickle bed reactor at 669 K, 51 atm, 1/1 CO/H₂ ratio and 668 (1/hr) space velocity.

The Selective Pathway to Higher Oxygenates from CO, H₂, Olefins, and Chlorocarbons

Raja Krishnamurthy, Steven S. C. Chuang*, Mark A. Brundage and Michael W. Balakos
Department of Chemical Engineering,
The University of Akron,
Akron, OH 44325-3906, U.S.A.

Keywords: CO insertion, Oxygenates, Reaction pathway, Transient kinetics.

The synthesis of higher oxygenates from CO hydrogenation, ethylene addition and methylene chloride addition to syngas has been studied over Rh/SiO₂ catalyst. The insertion of linear CO into the adsorbed alkyl intermediates is the key step in the formation of higher oxygenates. Pulse transient technique incorporated with *in situ* infrared (IR) technique reveals that hydrogenation of acyl species is the rate limiting step for propionaldehyde formation. Increasing total pressure increases the residence time of alkyl intermediates for CO insertion.

INTRODUCTION

The synthesis of higher oxygenates from CO and related reactions involves a number of elementary steps: (i) the formation of alkyl intermediates, (ii) the insertion of linear CO into the adsorbed alkyl intermediates to form acyl intermediates, and (iii) hydrogenation of the acyl intermediates (1-3). Figure 1 shows the possible reaction pathway for the formation of alkyl intermediates. Alkyl intermediates can be formed from (i) CO dissociation and hydrogenation in the CO and H₂ reaction (4,5), (ii) partial hydrogenation of an olefin, such as ethylene, in the CO/H₂/Olefin reaction (6), and (iii) dehalogenation of chloromethanes in the CO/H₂/CH_xCl_{4-x} reaction (7).

The selectivity towards oxygenates depends on the ratio of hydrogenation rate to the CO insertion rate. Design of a selective catalyst for C₂₊ oxygenate synthesis requires an understanding of the reactivity of alkyl group towards hydrogenation and CO insertion reaction steps. This paper reports the use of *in situ* IR and dynamic approach to study the nature of active sites and elementary steps involved in the higher oxygenate synthesis from CO/H₂ and CO/H₂/C₂H₄ reactions (8).

EXPERIMENTAL

Catalyst Preparation and Characterization

4 wt% Rh/SiO₂ catalyst was prepared from RhCl₃·3H₂O solution by incipient wetness impregnation method. After impregnation the catalyst was dried overnight in air at 300 K and then reduced in flowing hydrogen at 673 K for 16 hr. The exposed metal atoms was determined to be 244 μmol/g by H₂ pulse chemisorption at 303 K assuming an adsorption stoichiometry of H_{ads}/Rh = 1.

Reaction Studies

CO hydrogenation, ethylene addition, and methylene chloride addition were carried out in a differential reactor system. Space velocities of 11,000 h⁻¹ were used to keep the CO conversion below 5% in order to minimize heat and mass transfer effects and secondary reactions. Methylene chloride was added to the reactant gas mixture by bubbling hydrogen through a saturator filled with CH₂Cl₂ at 273 K. The product distribution was determined using a HP-5890A gas chromatograph (GC) with a 6 ft. Porapak PS column in series with a 6 ft. Porapak QS column.

Steady State Isotopic Pulse Transient Studies

The prepared catalyst was pressed into a self-supporting disk and placed in an IR reactor cell capable of operating up to 723 K and 6.0 MPa. The catalyst was further reduced *in situ* at 673 K for 1 hr before each experiment. Steady-state flow of CO/H₂ was admitted to the reactor. A 6-port GC

* Author to whom correspondence should be addressed

sampling valve was used to inject 10 cm³ of isotopic species into the steady-state CO flow which created a positive ¹³CO pulse and a negative ¹²CO pulse with symmetry as shown in Fig 2 (a). The symmetric response indicates that ¹²CO was replaced by ¹³CO at a 1 to 1 ratio and total CO (¹²CO and ¹³CO) flow was maintained at steady-state. It should be noted that proper balancing of ¹³CO pressure in the sampling loop and the ¹²CO flow line is essential for maintaining steady-state flow conditions. The reactant ¹²CO gas contains 2% Ar which is used to determine the effect of gas holdup in the reactor and the transportation lines on the transient response of gaseous products (Fig 2). Main components in the effluent of the IR cell were monitored by a mass spectrometer (MS). The change in the IR spectra of adsorbed species with time during the ¹³CO pulse was monitored by an FTIR spectrometer. The composition of the product gas was determined by the gas chromatograph.

RESULTS AND DISCUSSION

CO hydrogenation over Rh/SiO₂ produced methane as major product and C₂-C₅ hydrocarbons as minor products in the temperature range of 473 - 573 K and 0.1 MPa. No oxygenated product was produced at 0.1 MPa. Increasing reaction pressure to 0.4 MPa led to the formation of acetaldehyde. The higher oxygenate selectivity increases with reaction pressure (8). The effect of reaction pressure on oxygenate selectivity was studied by steady-state isotopic pulse transient. Residence time of reactants in the reactor cell for the 0.4 MPa runs was kept the same as for the 0.1 MPa runs by increasing the total flow rate from 60 cm³/min to 240 cm³/min.

The responses of ¹³CH₄ and CH₃¹³CHO to ¹³CO pulse at 0.1 MPa and 0.4 MPa are shown in Figure 2 (a) and (b). The residence time, τ , of intermediate to products is determined by the following equation (9)

$$\tau = \int_0^{\infty} tE(t)dt - \tau_r$$

τ for methane was determined to be 0.14 and 0.54 min for CO hydrogenation at 0.1 MPa and 0.4 MPa, respectively. Increasing reaction pressure increased the τ for CH₄ suggesting that CH_x for hydrogenation stays on the surface longer at high pressure than at low pressure. τ for CH₃CHO is smaller than that for CH₄ at 0.4 MPa. Formation of acetaldehyde at high reaction pressure can be explained by the increase in residence time of CH_x intermediates at high CO/H₂ pressure allowing CO insertion to occur.

An alternate approach to increase C₂ oxygenate selectivity is to increase the surface concentration of alkyl intermediates. Addition of CH₂Cl₂ to CO/H₂ has been found to result in the formation of acetaldehyde on Rh/SiO₂ and Ni/SiO₂ at 0.1 MPa (10,11). Increasing methyl concentration accelerates the rate of CO insertion resulting in the formation of C₂ oxygenates. Such a process even occurs on Ni/SiO₂, which exhibits little CO insertion activity during CO hydrogenation. Increasing ethyl intermediate concentration by the addition of ethylene to CO/H₂ over Ni/SiO₂ can also lead to the formation of propionaldehyde, the product of CO insertion (12). The mechanism of the formation of propionaldehyde from CO/H₂/C₂H₄ was further studied by isotopic pulse transient technique over Rh/SiO₂.

Figure 3 shows a response of a 10 cm³ pulse of ¹³CO into ¹²CO/Ar flow at 0.1 MPa and 503 K during the CO/H₂/C₂H₄ reaction. The figure shows the transient response for Ar, ¹²CO, ¹³CO, and C₂H₅¹³CHO. The symmetrical nature of the ¹²CO and ¹³CO response indicates that the species displaced each other and the total concentration of CO, isotopic and non-isotopic, remained the same during the pulse. Steady-state reaction conditions were maintained during the isotopic pulse transient study. The lag time between the argon and the CO response is due to the interaction of the gas phase CO with the adsorbed CO, i.e., adsorption and desorption effects. The time delay in the ¹³C propionaldehyde response corresponds to the residence time of the ¹³C surface intermediates leading to the formation of propionaldehyde. Modeling results reveal that the hydrogenation of the acyl intermediate is the rate-determining step for the formation of propionaldehyde (13).

CONCLUSION

The higher oxygenate formation on Rh catalysts involve a key CO insertion step. The linearly adsorbed CO is inserted into the adsorbed hydrocarbon intermediate formed from reaction of chlorinated hydrocarbons and ethylene and CO hydrogenation. Hydrogenation of the acyl intermediate is the rate-determining step for the formation of propionaldehyde from CO/H₂/C₂H₄. The higher oxygenates selectivity can be increased by increasing reaction pressure during CO hydrogenation, and addition of CH₂Cl₂ and C₂H₄.

REFERENCES

1. Chuang, S. C., Tian, Y. H., and Goodwin, J. G., Jr., *J. Catal.*, 96, 449 (1985).
2. Chuang, S. S. C., and Pien, S. I., *J. Catal.*, 138, 536 (1992).
3. Chuang, S. S. C., Pien, S. I., and Narayanan, R., *Appl. Catal.*, 57, 241 (1990).
4. Bell, A. T., *Catal. Rev. Sci. Eng.*, 23, 203 (1981).
5. Biloen, P., and Sachtler, W. M. H., *Adv. Catal.*, 30, 165 (1981).
6. Chuang, S. S. C., and Pien, S. I., *J. Catal.*, 135, 618 (1992).
7. van Barneveld, W. A. A., Ph. D. Thesis, University of Leiden, Netherlands, 1985.
8. Chuang, S. C., Goodwin, J. G., Jr., and Wender, I., *J. Catal.*, 95, 435 (1985).
9. Srinivas, G., Chuang, S. S. C., and Debnath, S., *J. Catal.*, in press.
10. Srinivas, G., M. S. Thesis, The University of Akron, Akron, 1991.
11. Balakos, M. W., Chuang, S. S. C., Krishnamurthy, R., and Srinivas, G., *Proceedings of the 10th International Congress on Catalysis, Part B*, (L. Guzzi, F. Solymosi, and P. Tetenyi, Eds.), Elsevier Science Publishers, Amsterdam, p. 1467, 1993.
12. Chuang, S. S. C., and Pien, S. I., *Catal. Lett.*, 6, 389 (1990).
13. Balakos, M. W., and Chuang, S. S. C., *J. Catal.* (submitted).

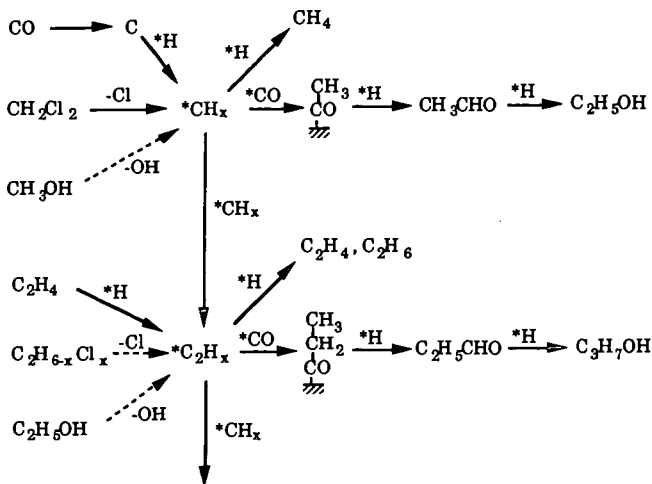


Figure 1. Proposed reaction pathway for syngas related reactions.

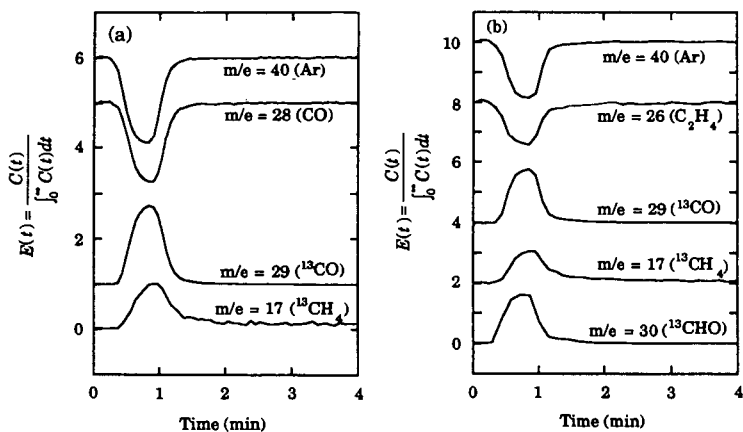


Figure 2. MS response to ^{13}CO pulse in CO/H_2 on $\text{Rh}(\text{Cl})/\text{SiO}_2$ at 543 K and (a) 0.1 MPa and (b) 0.4 MPa.

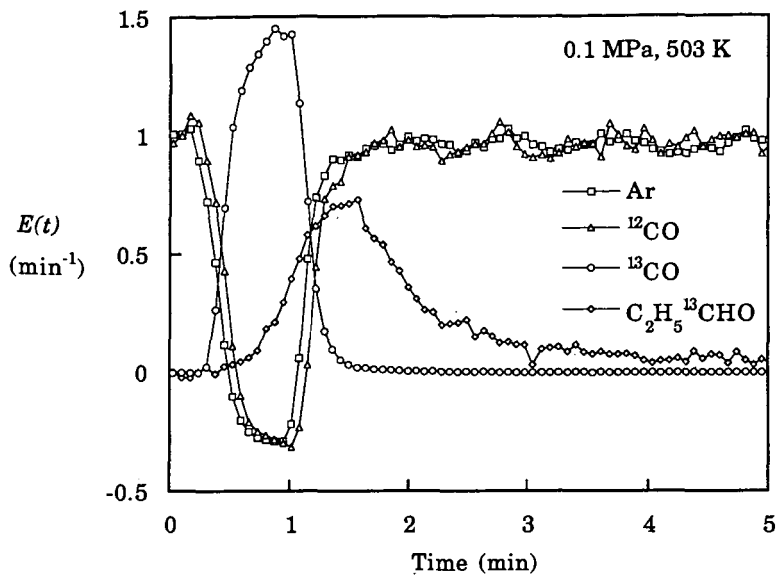


Figure 3. Transient response of Ar, ^{13}CO , and $\text{C}_2\text{H}_5^{13}\text{CHO}$ to a pulse of ^{13}CO in ^{12}CO flow during ethylene hydroformylation on 4 wt% Rh/SiO₂ at 503 K and 0.1 MPa

ISOBUTANOL COUPLING WITH ETHANOL AND METHANOL TO ETHERS OVER SULFONATED RESIN CATALYSTS: ACTIVITIES AND SELECTIVITIES

Richard G. Herman, Kamil Klier, Owen C. Feeley,
Marie A. Johansson, Qun Sun, and Luca Lietti
Zettlemoyer Center for Surface Studies and Department of Chemistry
7 Asa Drive, LEHIGH UNIVERSITY, Bethlehem, PA 18015

Keywords: Alcohols, Ethers, Resin Catalysts

ABSTRACT

The synthesis of C₃-C₈ ethers from mixtures of C₁-C₄ alcohols over strong acid Amberlyst resin catalysts has been initiated, and the overall activity pattern of the resins was found to be Amberlyst-35 > Amberlyst-36 > Amberlyst-15 > Amberlyst-1010, all of which were more active than Nafion-H. With methanol/isobutanol reactants, it was observed that increasing the reaction pressure strongly decreased the space time yield and selectivity of the butenes, principally isobutene, while tending to increase the space time yield of the ethers methylisobutylether (MIBE), methyl tertiarybutyl ether (MTBE), and dimethylether (DME). Other reactant mixtures utilized at high flow rates included ethanol/isobutanol, where EIBE and ETBE were products. Upon increasing the isobutanol/ethanol ratio above 1/1, it was shown that diethylether (DEE) formation decreased but the synthesis of tertiarybutyl isobutylether (TBIBE) increased. A reactant mixture of ethanol/isopropanol was also investigated, and dehydration of the isopropanol readily occurred to form propene and coupling gave diisopropylether (DIPE) as the dominant product at 90°C.

INTRODUCTION

The objective of this research program is to explore new pathways for synthesizing high value oxygenates, e.g. fuel-grade ethers, from non-petroleum feedstocks. In particular, the development of catalysts and processes for converting alcohols produced from coal- or natural gas-derived H₂/CO/CO₂ synthesis gas is being pursued. Alkali-doped Cu/ZnO-based catalysts produce a mixture of alcohols from H₂/CO, and this mixture consists principally of methanol and isobutanol [1-6]. The synthesis of ethers from these two alcohols has been shown to occur by the direct coupling of methanol and isobutanol over strong acid catalysts, and the observed dominant products were MIBE at moderate pressures and a mixture of methanol and isobutene at low pressures [7,8]. This research has now been extended to ethers containing the ethyl and isopropyl groups instead of the methyl moiety.

EXPERIMENTAL

The Amberlyst solid acid resin catalysts, designated as Amberlyst-15, -35, -36, and -1010, were obtained from Rohm and Haas. These catalysts have similar polymeric structures, but the Amberlyst-35 and -36 resins are more thermally stable (up to ≈140°C) and have higher acidity (5.2 and 5.4 meq/g dry, respectively) than the commonly utilized Amberlyst-15 resin (4.7 meq/g dry), while the Amberlyst-1010 has a much higher surface area (≈540 m²/g), smaller average pore size (5 nm rather than 20-30 nm), and lower concentration of acid sites (3.3 meq/g dry). Aqueous ion exchange titrations here with 0.5 NaOH confirmed the number of acid sites as stated by the manufacturer. The swelling properties of the dried (to 90°C) resins in water and in methanol were also determined, and it was observed that the Amberlyst-15, -35, and -36 resins swelled 42-58%, while the Amberlyst-1010 swelled 22-25% (the two liquids induced similar swelling behavior).

The catalysts were subjected to a standard test for ether synthesis in a downflow stainless steel bench-scale reactor system that is automated for continuous operation, as previously described [9,10]. The alcohols were injected at the top of the reactor in a preheated zone by means of a high pressure Gilson pump and an ISCO piston pump provided by Air Products and Chemicals, Inc. The carrier gas consisted of He containing 18.5% of N₂. The conversion and product composition were monitored by continual sampling of the exit stream by GC analysis using in-line, heated, automated Valco sampling valves [10]. The initial experimental conditions are as follows:

Catalyst weight	5.0 g dry resin	Methanol feed	1.72 mol/kg cat/hr
Temperature	90°C	Isobutanol feed	1.72 mol/kg cat/hr
Total pressure	1 atm (0.1 MPa)	He/N ₂ carrier	16 mol/kg cat/hr

RESULTS

Activities and Selectivities of the Amberlyst Catalysts. Testing of the catalysts was carried out under steady state conditions at each temperature, and the data were tabulated as averages during 3-15 hr runs for each set of reaction parameters. Comparison of the conversions of the alcohols at 90°C is made in Table 1. Upon increasing the reaction temperature sequentially in 10°C increments to 130°C, the activity increased with each catalyst. Since the Amberlyst-35 resin was the most active catalyst, the stability of the catalyst was investigated. Table 2 shows that no deactivation was observed during this 50 hr test, and, therefore, testing at 130°C did not cause destruction nor fouling of the resin.

Selectivity data were compiled for all catalytic tests, but only those for the Amberlyst-35 catalyst will be presented here. Under the reaction conditions employed, the catalysts were generally rather non-selective, especially at the lower temperatures. The Amberlyst-1010 tended to exhibit higher selectivity toward DME than did the other Amberlyst resins. As shown in Figure 1, Amberlyst-35 mainly formed butenes at 90-110°C, but at 120°C and above DME was predominantly formed.

Pressure Dependence Study of Amberlyst-35. The reaction of methanol and isobutanol over a Nafion-H catalyst has previously been shown to be very sensitive to the total pressure [7,8]. To investigate the pressure dependence of the synthesis reaction over Amberlyst-type catalysts, the active Amberlyst-35 resin was chosen. The total reaction pressure was varying while maintaining a constant reactant flow rate. The experiment was carried out using the following conditions:

Catalyst weight	1.0 g dry catalyst	Methanol feed	10.4 mol/kg cat/hr
Temperature	90 and 117°C	Isobutanol feed	5.2 mol/kg cat/hr
Total pressure at		He + N ₂	185 mol/kg cat/hr
90°C	0-79 psig (0.1-0.64 MPa)		
117°C	0-180 psig (0.1-1.3 MPa)		

Similar trends in selectivities were observed for the two reaction temperatures, and demonstrated that the formation of butenes (generally ≈85% of the butenes consisted of isobutene) was very sensitive to the alcohol partial pressure, e.g. Figure 2. Thus, a small elevation of the alcohol pressure suppressed the formation of butenes rather drastically, while the synthesis rates of DME, MIBE, and MTBE ethers were affected much less significantly, although there was a trend to increase the space time yield of these ethers as the alcohol pressure was increased.

Coupling Reactions of Ethanol with Isobutanol and Isopropanol. The coupling reactions of ethanol with isobutanol and isopropanol were investigated over the Amberlyst-35 catalyst at 90°C and 1 MPa under a wide range of conditions; in particular the relatively low conversion levels were usually maintained so that the data could subsequently be incorporated into a kinetic and mechanistic model of ether synthesis over this catalyst. The lower conversion levels were achieved by utilizing high GHSV.

Table 3 shows the conversions and product selectivities from ethanol/isobutanol = 1/1 and 1/3 reactant mixtures at 110°C. The higher level of isobutanol tended to decrease the overall alcohol conversion and the selectivity toward DEE. However, it significantly increased the selectivity toward the formation of TBIBE. Decreasing the ethanol/isobutanol ratio to 1/5 and the temperature to 100°C decreased the reaction rates even more but increased the selectivity to TBIBE, as well as of the isobutene (Table 4). For comparison, the data obtained for the methanol/isobutanol reaction at 110°C are shown in Table 5. Similar selectivity trends are noted by comparing Tables 3 and 5.

Studies have also been carried out with ethanol/isopropanol reactant mixtures at high flow rates, and an example of the data is given in Table 6. It is evident that isopropanol is quite reactive, in particular with respect to dehydration to form propene and DIPE, which has a blending octane number of 105 [10]. In addition, much more ethylisopropylether (EIPE) than DEE is formed. It is expected that high yields of these ethers could be formed by using much lower gas flow rates.

CONCLUSIONS

The strong acid Amberlyst resins are active for the synthesis of ethers and olefins from mixtures of alcohols. With the exception of Amberlyst-36, the activity of the macro-

reticular Amberlyst catalysts at 90°C correlated with the content of the strong acid sites, with Amberlyst-35 being the most active, and differences in selectivity patterns were observed. With methanol, ether products consisted of DME, MIBE, MTBE, and isobutene (with ethanol, analogous ethyl products were formed), and it was shown that increasing reaction pressure greatly decreased the selectivity toward isobutene. With ethanol/isobutanol reactants at 1 MPa over Amberlyst-35, tertiarybutylisobutylether (TBIBE) was a significant product, and this ether should have desirable fuel properties. In an experiment with ethanol/isopropanol = 1/1.6 reactants, it was shown that isopropanol was more reactive than ethanol and formed propene and DIPE, as well as EIPE.

ACKNOWLEDGEMENT

This research was partially supported by the U.S. Department of Energy (Pittsburgh Energy Technology Center), in part under Contract No. DE-AC22-90PC90044 and in part as a DOE Subcontract through Air Products and Chemicals, Inc.

REFERENCES

1. Klier, K., Herman, R. G., and Young, C.-W., *Preprints, Div. Fuel Chem., ACS*, 29(5), 273 (1984).
2. Klier, K., Herman, R. G., Nunan, J. G., Smith, K. J., Bogdan, C. E., Young, C.-W., and Santiesteban, J. G., in "*Methane Conversion*," ed. by D. M. Bibby, C. D. Chang, R. F. Howe, and S. Yurchak, Elsevier, Amsterdam, 109 (1988).
3. Nunan, J. G., Bogdan, C. E., Klier, K., Smith, K. J., Young, C.-W., and Herman, R. G., *J. Catal.*, 116, 195 (1989).
4. Nunan, J. G., Herman, R. G., and Klier, K., *J. Catal.*, 116, 222 (1989).
5. Herman, R. G., in "*New Trends in CO Activation*," ed. by L. Guzzi, Elsevier, Amsterdam, 265 (1991).
6. Herman, R. G., Klier, K., Young, C.-W., Nunan, J. G., Feeley, O. C., and Johansson, M. A., *Proc. 9th Intern. Pittsburgh Coal Conference*, 409 (1992).
7. Nunan, J., Klier, K., and Herman, R. G., *J. Chem. Soc., Chem. Commun.* (1985) 676.
8. Nunan, J. G., Klier, K., and Herman, R. G., *J. Catal.*, 139 (1993) 406.
9. Klier, K., Herman, R. G., Johansson, M. A., and Feeley, O. C., *Preprints, Div. Fuel Chem., ACS*, 37(1), 236 (1992).
10. Herman, R. G., Klier, K., Feeley, O. C., and Johansson, M. A., *Preprints, Div. Fuel Chem., ACS*, 39(2), 343 (1994).

TABLE 1. Activity of the polymeric resin catalysts at 90°C

Catalyst	% Methanol Conversion	% Isobutanol Conversion
Amberlyst-15	9.1	10.2
Amberlyst-35	16.4	15.8
Amberlyst-36	12.3	10.2
Amberlyst-1010	5.0	4.2

TABLE 2. Amberlyst-35 activity as a function of reaction temperature.

Temperature (°C)	% Methanol Conversion	% Isobutanol Conversion
90	16.4	15.8
100	32.1	43.9
110	42.9	63.9
120	62.0	57.1
130	70.0	57.9
90	17.0	15.7

TABLE 3. Activity and selectivity for the conversion of ethanol and isobutanol (10.3/10.4 and 10.3/31.2 mol/kg cat/hr) to products over the Amberlyst-35 catalyst (1 g) at 110°C and 1.1 MPa with total flow rate of 516 mol/kg cat/hr

Product	Conversion (mol%)	Selectivity (%) Based on Ethanol	Selectivity (%) Based on Isobutanol
Ethanol	12.3, 7.4		
Isobutanol	10.2, 4.1		
DEE		63.1, 42.7	
ETBE		2.1, 4.0	2.5, 2.3
EIBE		34.8, 53.4	41.4, 31.2
Isobutene			37.9, 33.9
TBIBE			8.6, 22.0
DIBE			5.8, 7.4

TABLE 4. Activity and selectivity for the conversion of ethanol and isobutanol (14/69 mol/kg cat/hr) to products over the Amberlyst-35 catalyst (0.5 g) at 100°C and 1.1 MPa with total flow rate of 575 mol/kg cat/hr

Product	Conversion (mol%)	Selectivity (%) Based on Ethanol	Selectivity (%) Based on Isobutanol
Ethanol	1.7		
Isobutanol	1.8		
DEE		16.6	
ETBE		5.2	1.2
EIBE		78.2	17.7
Isobutene			42.1
TBIBE			29.0
DIBE			10.0

TABLE 5. Activity and selectivity for the conversion of methanol and isobutanol (22.8/26.0 and 7.6/26.0 mol/kg cat/hr) to products over the Amberlyst-35 catalyst (1 g) at 110°C and 1.1 MPa with total flow rate of 524 mol/kg cat/hr

Product	Conversion (mol%)	Selectivity (%) Based on Methanol	Selectivity (%) Based on Isobutanol
Methanol	8.3, 9.8		
Isobutanol	4.3, 5.8		
DME		63.9, 38.0	
MTBE		3.7, 8.1	6.3, 4.0
MIBE		32.4, 53.9	55.7, 26.62
Isobutene			18.2, 39.8
TBIBE			12.4, 21.0
DIBE			7.4, 8.6

TABLE 6. Activity and selectivity for the conversion of ethanol and isopropanol (40/64 mol/kg cat/hr) to products over the Amberlyst-35 catalyst (0.5 g) at 90°C and 1.1 MPa with total flow rate of 596 mol/kg cat/hr

Product	Conversion (mol%)	Selectivity (%) Based on Methanol	Selectivity (%) Based on Isobutanol
Ethanol	1.4		
Isopropanol	4.0		
DEE		14.4	
EIPE		85.6	18.4
Propene			32.1
DIPE			49.5

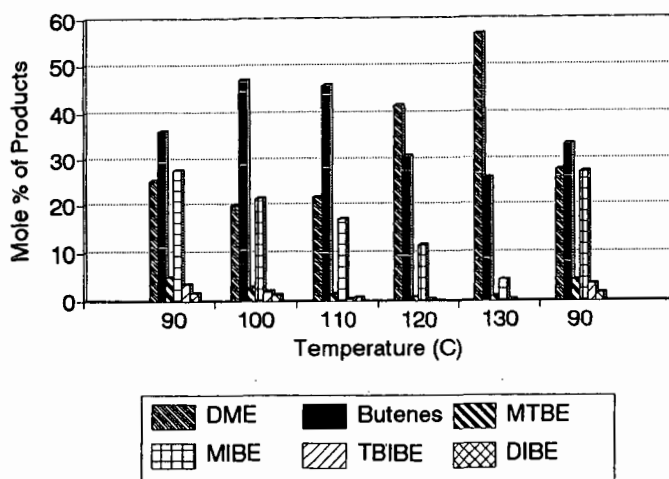


FIGURE 1. The selectivities of the products formed at different temperatures over the Amberlyst-35 resin at 0.1 MPa from a methanol/isobutanol = 1/1 reactant mixture.

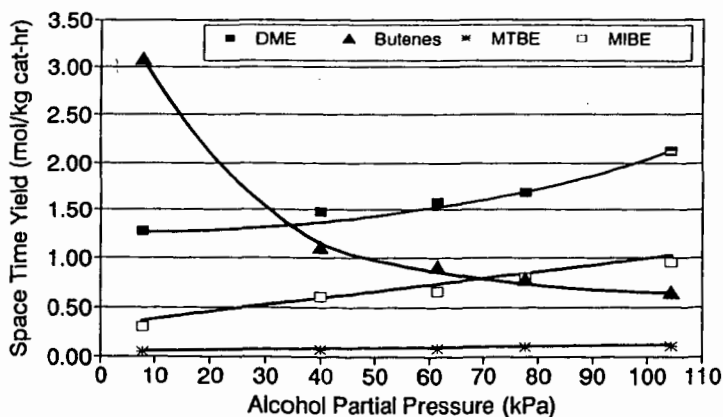


FIGURE 2. Space time yields of the ethers and butenes (mainly isobutene, but also including *trans*-2-butene and *cis*-2-butene) formed over the Amberlyst-35 catalyst as a function of the alcohol partial pressure at 117°C (methanol/isobutanol = 2/1).